文章编号：1001-9014(2021)03-0302-06

DOI:10.11972/j.issn.1001-9014.2021.03.004

Temperature-dependent photoresponse of monolayer MoS_2 film grown by pulsed laser deposition

XIE Ming-Zhang[1], LI Liu-Meng[1], LI Ming[1], YE Yan[1], ZHANG Jin-Zhong[1], JIANG Kai[1], SHANG Li-Yan[1], HU Zhi-Gao[1,2*], CHU Jun-Hao[1,2]

(1. Technical Center for Multifunctional Magneto-Optical Spectroscopy (Shanghai), Engineering Research; Center of Nanophotonics & Advanced Instrument (Ministry of Education), Department of Materials, School of Physics and Electronic Science, East China Normal University, Shanghai 200241, China;
2. Shanghai Institute of Intelligent Electronics & Systems, Fudan University, Shanghai 200433, China)

Abstract: We report the preparation and photoresponse of MoS_2 films with different layers grown on c-Al_2O_3 by pulsed laser deposition (PLD). The phonon modes and crystallographic orientation discussed by Raman scattering and X-ray diffraction (XRD) prove that the MoS_2 films are of pure 2H-phase. The S/Mo ratio of film is identified as 1.92:1 derived by X-ray photoelectron (XPS) experiments. The blue and red shifts of the Mo 3d peaks for XPS data indicate the existence of oxidation and sulfur defects in the films. Moreover, by Raman and photoluminescence (PL) mapping, the film thickness is proven to be uniform. The temperature-dependent photoresponse of monolayer MoS_2 film indicates that the temperature plays an important role in the photoresponse intensity and response time. The present results can provide a reference for further improving the performance of MoS_2-based photodetectors.

Key words: molybdenum disulfide, pulsed laser deposition, photoluminescence, photoresponse

脉冲激光沉积法制备的单层 MoS_2 薄膜变温光响应研究

谢明章[1], 李留猛[1], 李 明[1], 叶 艳[1], 张金中[1], 姜 凯[1], 商丽燕[1], 胡志高[1,2*], 褚君浩[1,2]

(1. 华东师范大学 物理与电子科学学院,材料科学系,纳光电集成与先进装备教育部工程研究中心,上海市极化材料多功能磁光光谱技术服务平台,上海 200241;
2. 复旦大学 上海智能电子与系统研究院,上海 200433)

摘要:报导了在 c-Al_2O_3 衬底上用脉冲激光沉积法制备 MoS_2 薄膜,并测试了其不同温度下的光响应。通过拉曼散射光谱和X射线衍射光谱证明了所制备的二硫化钼为纯2H相。通过X光电子能谱证明了所制备的二硫化钼硫钼原子比为1.92:1,在Mo元素的3d核心能级谱中存在红移和蓝移,说明薄膜中存在氧化和硫缺陷。此外,通过拉曼和光致发光分布图,证明了薄膜具有良好的均一性。在不同层数的二硫化钼样品中,单层二硫化钼样品具有最强的光响应,达到3 mAW^{-1}。单层二硫化钼的变温光响应实验表明,在室温附近,温度升高会提高二硫化钼的光响应强度和响应时间。

关 键 词:二硫化钼;脉冲激光沉积;光致发光;光响应

中图分类号:O43　　**文献标识码**:A

Received date: 2020-08-02, **revised date**: 2021-03-09　　**收稿日期**:2020-08-02,**修回日期**:2021-03-09

Foundation items: Supported by the National Key R&D Program of China (2018YFB0406500, 2019YFB2203400); the Natural Science Foundation of China (91833303, 61974043, 61674057); Projects of Science and Technology Commission of Shanghai Municipality (18JC1412400, 18YF1407200, 18YF1407000, 19511120100).

Biography: XIE Ming-Zhang (1990-), Male, Shanghai, Ph. D. Research area involves 2D materials and devices. E-mail: 52161213017@stu.ecnu.edu.cn

* **Corresponding author**: E-mail: zghu@ee.ecnu.edu.cn

Introduction

Since graphene has been found, two-dimensional materials as promising materials for next-generation semiconductor devices have been studied and applied in many fields. Among them, transition metal dichalcogenides (TMDs) materials attracted lots of attention with their unique properties[1-2]. MoS_2 was one of the TMDS with a direct band gap of about 1.9 eV in monolayer and an indirect bandgap of about 1.3 eV in bulk, which makes it possible in optoelectronic applications[3-4].

As we know, optoelectronic devices have a wide range of applications in every corner of life, such as photodetectors, solar cells, and light-emitting diodes. The thickness of monolayer MoS_2 is less than 1 nm, which can be applied in low-dimensional optoelectronic devices. Although chemical vapor deposition (CVD) is the most widely used method for growing two-dimensional materials, other alternative methods are employed at the same time, such as magnetron sputtering[5], atomic layer deposition[6], spin-coating[7], and so on. The pulsed laser deposition (PLD) method can prepare films with the same stoichiometric ratio as the target[8]. As one of the physical vapor deposition methods, PLD was also tried to fabricate large-scale, high-crystallinity and stable-output MoS_2 and other 2D films. Many previous work has proved PLD is a practical method for growing two-dimensional materials[9-14].

Sapphire is a commonly used insulating substrate with good optical, mechanical properties and chemical stability. Growing MoS_2 films on sapphire substrates is valuable for applications of MoS_2. Xu et al. reported wafer-scale MoS_2 films on sapphire substrates prepared by a two-step vapor-solid phase reaction process and focused on their electrical performance[15]. Also, some people have employed PLD to grow MoS_2 films on sapphire substrates directly and studied their morphology and structure, but not paying attention to the photoresponse[16-17]. Jiao et al. reported preparing high quality MoS_2 films with different thicknesses by PLD and investigated the layer-dependent photoresponse ranging from UV-visible-NIR spectra[18], but the influence of temperature is not considered. Note that, the temperature affects the stability of the device operation. As we know, temperature will cause the expansion or contraction of the crystal lattice, which will change the phonon vibration and electronic structure of the crystal[19-20]. We think this will affect the photoelectric properties of the crystal. If the MoS_2 films are to be used in optoelectronic devices, the effects on the photoresponse from the temperature must be considered. Studying the effects of temperature on photoresponsivity and response time is necessary. Therefore, in this paper, we prepared MoS_2 films with different layers directly using PLD technology. Then, we investigated the structure, composition, uniformity and the photoresponse in different situations.

1 Experiments

A commercial target was placed 5.5 cm in front of the substrates with S/Mo ratio of 2:1. A pulsed 248 nm KrF excimer laser was used to etch the surface of the target. The energy fluence is set to 4 Jcm^{-2} with a repetition rate of 5 Hz. Before placed in the vacuum chamber, the square sapphire substrates with a thickness of 0.5 mm were cleaned in alcohol, acetone, and deionized water for 15 minutes separately, combined with sonication. During the deposition, the chamber was kept at a vacuum of 5×10^{-6} mba. Simultaneously, the heater was kept at 800 ℃ and rotated to improve the flatness of the films. The thicknesses of the films are controlled by the repetition number of the laser pulses. Due to the volatility of sulfur, each sample was immediately placed in a double-temperature zone tube furnace and annealed in a sulfur atmosphere after being taken out of the PLD vacuum chamber. During the annealing progress, the samples were heated at 700 ℃ and the excess sulfur was heated at 200 ℃ with an argon flow rate of 100 sccm.

The thickness and the roughness were identified by atomic force microscopy (AFM, digital Instruments Icon, Bruker). The phonon changes and photoluminescence of the samples were studied by Raman spectroscopy (Jobin-Yvon LabRAM HR Evolution) using a 50× lens with an excitation laser beam wavelength of 532 nm. X-ray photoelectron spectroscopy (XPS, RBD upgraded PHI-5000C ESCA system, PerkinElmer) measurements were applied to investigate the Mo 3d and S 2p regions of the samples. X-ray diffraction (XRD, D/MAX-2550 V, Rigaku Co) analysis was carried out to investigate the crystalline and compositions. The electrical characteristics and photoresponse were measured by a Keithley model 4200 with gold contacts. A 637nm laser was used as the light source.

2 Results and discussions

2.1 Morphology and structure

Firstly, the surface morphology was measured by atomic force microscopy (AFM). Figure 1(a) shows the topography of a MoS_2 film deposited on a c-Al_2O_3 substrate. The calculated arithmetic roughness is 0.162 nm, which means that the film has extremely high flatness. The diffraction pattern in Fig. 1(b) for the film has five strong peaks at 14.4°, 29.1°, 41.8°, 44.2° and 60.1°. In addition to the peak at 41.8° belonging to the sapphire substrate, the other four peaks correspond to the (002) (004) (006) and (008) orientations (JCPDS No. 37-1492) of 2H-MoS_2, respectively. Besides, there are no peaks belonging to 1T-MoS_2. The full width at half maximum (FWHM) of (002) peak is 0.321°, which indicates that the crystallite size of this sample is 25.3 nm estimated by Scherrer formula [$D=0.9\lambda/(\beta\cos\theta)$]. From the Raman spectra in Fig. 1(c), except for the peaks derived from the substrate, the other 3 main peaks are the in-plane vibration E^1_{2g}, out-of-plane vibration A_{1g} and the second-order longitudinal acoustic mode at the M point 2LA(M). Note that the E^1_{2g} and A_{1g} modes are corresponding to the 2H-phase of MoS_2. Both the results of XRD and Raman spectra indicate that the MoS_2 films in this work is pure in 2H semiconductor phase[21]. A confo-

cal microscope system (Jobin-Yvon LabRAM HR Evolution spectrometer) with a 532 nm laser was adopted to collect the PL data of a film with 150 pulses. As shown in Fig. 1(d), a single strong excitonic peak appears around 665 nm corresponding to a band gap with 1.86 eV, the PL spectrum of sapphire is used as a reference, which suggests that it is a monolayer MoS_2 film.

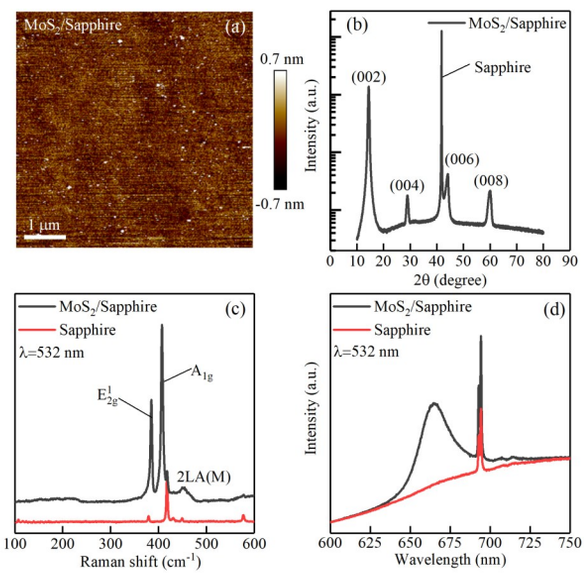

Fig. 1 (a) The AFM image of a MoS_2 film on a *c*-Al_2O_3 substrate, The (b) XRD and (c) Raman spectra of the MoS_2 film, (d) The PL spectra of a MoS_2 film

图1 (a)生长在氧化铝衬底上的二硫化钼薄膜的原子力显微镜图像,(b)X射线衍射光谱和(c)拉曼光谱图像,(d)二硫化钼的光致发光光谱

X-ray photoelectron spectroscopy (XPS) was used to analyze the stoichiometry and chemical states of the film. The spectra in Fig. 2 is referenced to C 1s emission at 284.6 eV. Fig. 2(a) is the survey spectra of the monolayer exhibit peaks for Mo and S elements as well as the sapphire substrate. Figure 2(b) and Figure 2(c) present the Mo and S core level peak regions, along with the deconvolutions of each spectrum. Some constraints are applied to ensure that the fitting results have a physical meaning. The binding energy differences ΔEB between Mo $3d^{5/2}$ and Mo $3d^{3/2}$ orbitals, S $2p^{3/2}$ and S $2p^{1/2}$ orbitals were constrained as (3.1±0.1)eV and (1.2±0.1) eV, respectively. The areas of Mo $3d^{5/2}$ and S $2p^{3/2}$ orbitals are constrained as 1.5 and 2 times of the Mo $3d^{3/2}$ and $2p^{1/2}$ orbitals, respectively[14,22]. As shown in Fig. 2(b), the strongest doublet peaks around 232.8 eV and 229.7 eV are attributed to the Mo^{4+} state of 2H MoS_2. The doublet peaks around 236.0 eV and 232.9 eV belong to Mo $3d^{3/2}$ and Mo $3d^{5/2}$ orbitals of Mo^{6+} state, which indicates the existence of oxidation. The peak around 226.9 eV is identified as S 2s core level. Additional doublet peaks around 232.1 eV and 229.0 eV red-shifted from the main peaks by 0.7 eV suggest the presence of Mo^{4+} of other states. Some works have reported that this phenomenon is due to the symbiosis of the 2H-phase and 1T-phase[23]. However, no evidence of the 1T-phase is found according to the results of Raman spectra and XRD. In this work, the sulfur defects reduce the actual valence of some Mo elements and increases the electron cloud density, which leads to a reduction in the binding energy of these Mo elements to the electrons[14,16,24]. For S 2p core level, the main peaks corresponding to $2p^{1/2}$ and $2p^{3/2}$ orbitals are around 163.7 eV and 162.5 eV. Similarly, there is a pair of doublet peaks around 162.8 eV and 161.6 eV red-shifted by 0.9 eV to the main peaks, indicating the presence of other S^{-2} states, which should be related to sulfur defects and oxidation. Through the areas of the S 2p peaks and Mo 3d peaks, the S/Mo ratio is calculated as 1.92:1.

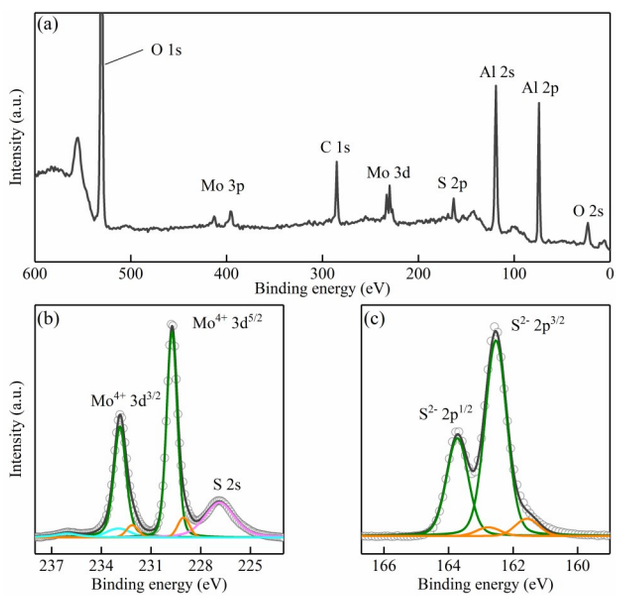

Fig. 2 (a) The survey XPS spectra of a film deposited for 150 pulses, The XPS spectra and its deconvolution of (b) Mo 3d and (c) S 2P core level

图2 (a)在150个脉冲沉积下的二硫化钼薄膜的光电子能谱,(b)钼的3d核心能级和(c)硫的2P核心能级光电子能谱及去卷积图像

2.2 Uniformity analysis

For two-dimensional materials, Raman mapping is often used to evaluate the uniformity of thin films[16,25-26]. As shown in Fig. 3(a), a random 40 μm × 40 μm area was tested for uniformity. The dark areas in the image may be related the particles sputtered from the target. The frequency difference ($\Delta\nu$) between the E^1_{2g} and A_{1g} modes of monolayer MoS_2, less than 20 cm^{-1}, is known as an indicator for monolayer. Therefore, Raman mapping was applied to measure the uniformity of the film. As shown in Fig. 3(b), most points in the picture have a frequency difference of less than 20 cm^{-1}. After calculation, the average value of the frequency difference is 19.7 cm^{-1} with the standard deviation of 0.35 cm^{-1}, which suggests that this film has a good uniformity in thickness. The intensity mapping of the A_{1g} mode is also presented in Fig. 3(c). The dispersion of the peak intensity is greater than the frequency difference, which may

be due to the difference in crystallinity introduced by defects, grain boundaries, impurities absorbed on surface, etc. At the same time, we suspect that the film is polycrystalline. Similar phenomena can also be found in PL mapping. In Fig. 3(d), the calculated average position value of the excitonic peak is 664.8 nm corresponding to a band gap of 1.87 eV, with a very small standard deviation of 0.29 nm. Similarly, the distribution of the PL intensity in Fig. 3(e) is not as even as the position, but with no dead pixels. Although the crystallinity distribution is not perfect, the MoS_2 films grown by PLD can be precisely controlled in thickness. Different layers of MoS_2 films were easily prepared, as shown in Fig. 3(f), which can be distinguished by the change in the frequency differences of the E^1_{2g} and A_{1g} modes. When the thickness increases, the E^1_{2g} shows a red shift and the A_{1g} modes has a blue shift, which is consistent with previous reports[26-27]. The inerlayer vdW interaction increasing the effective restoring forces acting on the atoms, which is believed to cause the blue shift of A_{1g} mode with increasing layer number. However, the red shift of E^1_{2g} mode may reflect the influence of stacking-induced structural changes, attributed to long-range Coulombic interlayer interaction[27]. Based on the XRD spectrum, Raman Spectrum, Raman and PL mapping, we speculate that the MoS_2 films grown by PLD in this work are pure in 2H-Phase and polycrystalline.

2.3 Effect of temperature

As for the optoelectronic properties, 40 nm thick gold electrodes were plated on the films using a mask by thermal evaporation to collect current. The channel between the adjacent electrodes is 50 μm wide and 150 μm long. Figure 4(a) shows the schematic of the photoresponse measurement progress. A 637 nm laser was used to excite the electron from valence band to conduction band. The photon energy of the selected laser is slightly larger than the band gap of monolayer MoS_2, so that it does not generate excessive heat under the premise that it can excite electrons from the valence band top to the conduction band bottom. This reduces the influence of the heat generated by the laser on the accuracy of temperature control. Figure 4(b) shows the layer-dependent time-resolved photocurrent of the MoS_2 films under the same laser irradiation and driving voltage. Compared the five films, the monolayer sample has a photocurrent of 0.32 nA with a photoresponsivity of about 3 mAW^{-1}, which is stronger than the others. As shown in Fig. 4(c), the layer-dependent rising (τ_{up}) and decay response times (τ_{down}) are extracted. The inset of Fig. 4(c) shows the rising and decay response times of the monolayer MoS_2 film. The monolayer MoS_2 film has the slowest response, which is believed to be related to its direct bandgap. When the number of layers increased to 2 or more layers, the direct bandgap becomes an indirect band gap, which reduces the photo-generated carrier life and response times. To further study the optoelectronic characteristics of the monolayer MoS_2 film, the photoresponse at different temperature under vacuum was carried out. Figure 4(d) shows the time-resolved photocurrent at 200 K, 270 K and 370 K. Each one shows good reproducibility at different temperatures after several cycles. The I_{photo} and I_{dark} increase synchronously with the temperature, as shown in Fig. 4(e). As the temperature increases, the intrinsic carrier concentration will increase with thermal excitation, which will increase the conductivity of monolayer MoS_2 film. So, the photocurrent and dark current both increase with the temperature, and the dark current is more affected by temperature. The study on tempera-

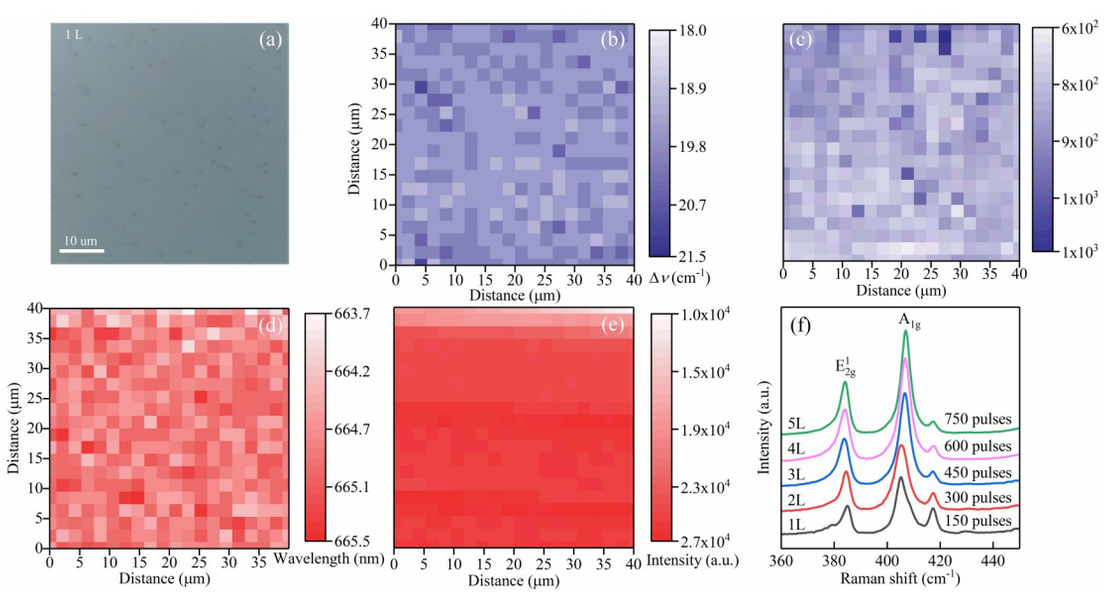

Fig. 3 (a) The optical image of a randomly selected 40 μm × 40 μm area, (b) The mapping of the frequency differences between E^1_{2g} and A_{1g} peaks, (c) The mapping of the intensity of the A_{1g} peak. The mapping of the excitonic peak (d) positions and (e) intensity, (f) The Raman spectra for different layers

图3 (a) 随机选取的40 μm×40 μm区域的单层二硫化钼的光学图像, (b) E12g和A1g峰之间频率差的分布图, (c) A1g峰强度分布图;光致发光激发峰(d)位置和(e)强度分布图,(f) 不同层数二硫化钼的拉曼图像

ture effects on the electronic structure found that the band gap will decrease monotonously with the temperature[20]. The narrowing of the band gap with the temperature will reduce the difficulty of electron excitation from valence band top to the conduction band bottom. As a result, the photocurrent of this monolayer MoS_2 film in the inset of Fig. 4(e) increases as the temperature rises. The τ_{up} and τ_{down} are extracted from the temperature-dependent photoresponse data, as shown in Fig. 4(f). When the temperature is lower than 260 K, the response time rises rapidly with the temperature. However, when the temperature is higher than about 280 K, the response time slows down as the temperature rises. The narrowing of the band gap with the temperature will decrease the response times. However, the ionization of defects will increase with temperature, becoming the scattering center of non-equilibrium carriers and increasing the lifetimes of the photo-generated non-equilibrium carriers, which will increase the response times. The change in response time around room temperature may be related to the complex competition between these mechanisms. Such results indicate that the temperature compensation needs to be considered when designing the MoS_2-based devices.

3 Conclusions

In conclusion, we prepared the high-quality and thickness-controllable MoS_2 films on the c-Al_2O_3 substrates using the PLD method. The phonon modes and crystallographic orientation were studied through Raman and XRD spectra, providing evidence for the pure 2H-phase. The XPS results show the existence of oxidation and sulfur defects in the films. By Raman and PL mapping, the thickness is proved good uniformity and the monolayer film is presumed to be polycrystalline. Moreover, we find that the temperature has a great influence on the optoelectronic properties. Our findings should be helpful for designing and producing high-performance MoS_2-based photodetectors.

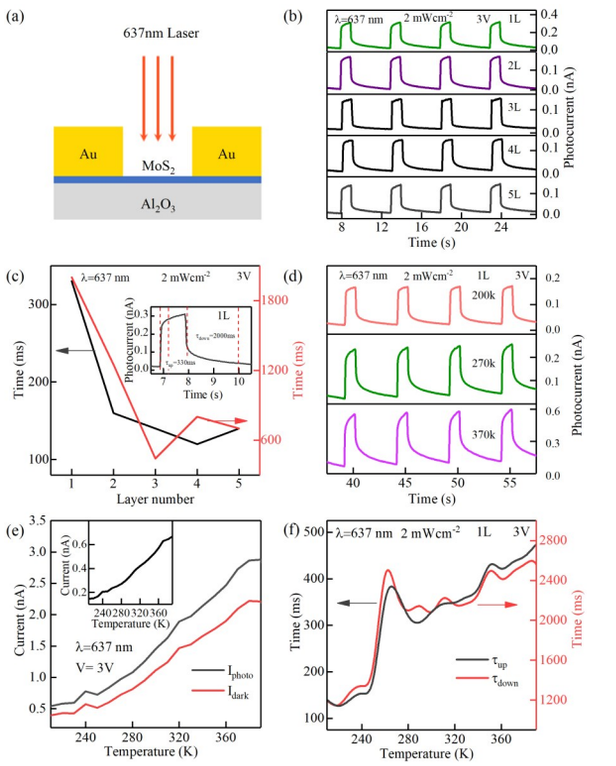

Fig. 4 (a) The schematic of the photoresponse measurement progress, (b) The time-resolved photocurrent of MoS_2 films with different layers, (c) The layer-dependent rising (τ_{up}) and decay response times (τ_{down}). The inset presents the rising and decay response times of the monolayer MoS_2 film, (d) The time-resolved photoresponse of a monolayer MoS_2 film at 200 K, 270 K and 370 K, (e) The temperature-dependent photoresponse of a monolayer MoS_2 film. The inset presents the temperature-dependent I_{ph}, (f) The temperature-dependent rising (τ_{up}) and decay response times (τ_{down})

图4 (a) 测试光响应的原理图,(b) 不同层数二硫化钼光电流的时间分辨光电流图像,(c) 不同层数的上升(τ_{up})和衰减时间(τ_{down}),(d) 200 K、270 K和370 K温度下单层二硫化钼薄膜的时间分辨光响应图像,(e) 单层二硫化钼薄膜的变温光响应图像,插图是不同温度的光生电流I_{ph},(f) 变温光响应的上升时间(τ_{up})和衰减时间(τ_{down})

References

[1] RADISAVLJEVIC B, RADENOVIC A, BRIVIO V, *et al*. Single-layer MoS_2 Transistors [J]. *Nature Nanotechnology*, 2011, **6**(3): 147-150.

[2] BHIMANAPATI G R, LIN Z, MEUNIER V, *et al*. Recent Advances in Two-dimensional Materials Beyond Graphene [J]. *ACS Nano*, 2015, **9**(12): 11509-11539.

[3] BURMAN D, GHOSH R, SANTRA S, *et al*. Role of Vacancy Sites and UV-ozone Treatment on Few Layered MoS_2 Nanoflakes for Toxic Gas Detection [J]. *Nanotechnology*, 2017, **28**(43), 435502-435518.

[4] WANG L, JIE J S, SHAO Z B, *et al*. MoS_2/Si Heterojunction with Vertically Standing Layered Structure for Ultrafast, High-detectivity, Self-driven Visible-Near Infrared Photodetectors [J]. *Advanced Functional Materials*, 2015, **25**(19):2910-2919.

[5] TAO J G, CHAI J W, LU X, *et al*. Growth of Wafer-scale MoS_2 Monolayer by Magnetron Sputtering [J]. *Nanoscale*, 2015, **7**(6): 2497-2503.

[6] TAN L K, LIU B, TENG J H, *et al*. Atomic layer deposition of a MoS_2 film [J]. *Nanoscale*, 2014, **6**(18): 10584-10588.

[7] YANG J, GU Y, LEE E, *et al*. Wafer-scale Synthesis of Thickness-controllable MoS_2 Films Via Solution-processing Using A Dimethylformamide/n-butylamine/2-aminoethanol Solvent System [J]. *Nanoscale* 2015, **7**(20): 9311-9319.

[8] YANG Z B, HAO J H. Progress in Pulsed Laser Deposited Two-dimensional Layered Materials for Device Applications [J]. *Journal of Materials Chemistry C*, 2016, **4**(38): 8859-8878.

[9] JIE W J, YANG Z B, ZHANG F, *et al*. Observation of Room-temperature Magnetoresistance in Monolayer MoS_2 by Ferromagnetic Gating [J]. *ACS Nano*, 2017, **11**(7): 6950-6958.

[10] XIE Y, ZHANG B, WANG S X, *et al*. Ultrabroadband MoS2 Photodetector with Spectral Response from 445 to 2 717 nm [J]. *Advanced Materials*, 2017, **29**(17):1605972-.

[11] GOSWAMI A, DHANDARIA P, PAL S, *et al*. Effect of Interface on Mid-infrared Photothermal Response of MoS_2 Thin Film Grown by Pulsed Laser Deposition [J]. *Nano Research*, 2017, **10**(10): 3571-3584.

[12] SERRAO C R, DIAMOND A M, HSU S L, *et al*. Highly Crystalline MoS_2 Thin Films Grown by Pulsed Laser Deposition [J]. *Applied Physics Letters*, 2015, **106**(5): 052101.

[13] ARULRAJ A, RAMESH M, SUBRAMANIAN, *et al*. In-situ Temperature and Thickness Control Grown 2D-MoS_2 via Pulsed Laser Ablation for Photovoltaic Devices [J]. *Solar Energy*, 2018, **174**(1): 286-295.

[14] LIU J, GOSWAMI A, JIANG K, *et al*. Direct-current Triboelectricity Generation by A Sliding Schottky Nanocontact on MoS_2 Multilayers [J]. *Nature Nanotechnology*, 2018, **13**(2): 112-116.

[15] XU X M, WANG Z W, LOPATIN S, *et al*. Wafer Scale Quasi Single Crystalline MoS_2 Realized by Epitaxial Phase Conversion [J]. *2D Ma-*

terials, 2018, **6**(1): 015030.
[16] SERNA M I, YOO S H, MORENO S, *et al*. Large-area Deposition of MoS_2 by Pulsed Laser Deposition with In Situ Thickness Control [J]. *ACS Nano*, 2016, **10**(6): 6054-6061.
[17] BARVAT A. PRAKASH N, SATPATI B, *et al*. Emerging Photoluminescence from Bilayer Large-area 2D MoS_2 Films Grown by Pulsed Laser Deposition on Different Substrates [J]. *Journal of Applied Physics*, 2017, **122**(1): 015304.
[18] JIAO L, JIE W J, YANG Z B, *et al*. Layer-dependent Photoresponse of 2D MoS2 Films Prepared by Pulsed Laser Deposition [J]. *Journal of Materials Chemistry C*, 2019, **7**(9): 2522-2529.
[19] LANZILLO N A, BIRDWELL A G, AMANI M, *et al*. Temperature-dependent phonon shifts in monolayer MoS2 [J]. *Applied Physics Letters*, 2015, **3**(5): 056103.
[20] MOLINA-SÁNCHEZ A, PALUMMO M, MARNI A, *et al*. Temperature-dependent excitonic effects in the optical properties of single-layer MoS2 [J]. *Physical Review B*, 2016, **93**(15): 155435.
[21] YU Y F, NAM G H, HE Q Y, *et al*. High Phase-purity 1T′-MoS_2- and 1T′-$MoSe_2$-layered Crystals [J]. *Nature Chemistry*, 2018, **10**(6): 638-643.
[22] LATE D J, SHAIKH P A, KHARE R, *et al*. Pulsed Laser-deposited MoS2 Thin Films on W and Si: Field Emission and Photoresponse Studies [J]. *ACS Applied Materials & Interfaces*, 2014, **6**(18): 15881-15888.
[23] BARVAT A, PRAKASH N, KUMAR G, *et al*. Electronic Structure of The PLD Grown Mixed Phase MoS_2/GaN Interface and Its Thermal Annealing Effect [J]. *Current Applied Physics*, 2018, **18**(2): 170-177.
[24] ZHANG X K, LIAO Q L, LIU S, *et al*. Poly(4-styrenesulfonate)-induced Sulfur Vacancy Self-healing Strategy for Monolayer MoS_2 Homojunction Photodiode [J]. *Nature Communications*, 2017, **8**(1): 15881.
[25] SEO S, KIM S, CHOI H, *et al*. Direct in Situ Growth of Centimeter-Scale Multi-Heterojunction MoS_2/WS_2/WSe_2 Thin-film Catalyst for Photo-electrochemical Hydrogen Evolution [J]. *Advanced Science*, **6**(13): 1900301.
[26] SIEGEL G, SUBBAIAH Y P V, PRESTGARD M C, *et al*. Growth of Centimeter-scale Atomically Thin MoS_2 Films by Pulsed Laser Deposition [J]. *APL Materials*, 2015, **3**(5):056103.
[27] LEE C G, YAN H G, BRUS L E, *et al*. Anomalous Lattice Vibrations of Single- and Few-Layer MoS2 [J]. *ACS Nano*, 2010, **4**(5): 2695-2700.